Journal of Engineering Science and Technology Review 17 (5) (2024) 126-134

Research Article

JOURNAL OF
Engineering Science
and Technology Review

www.jestr.org

Modified MBOC Modulation for GPS/Galileo Satellite Communication Systems

Mustapha Flissi[1,*], Salim Atia[1], Khaled Rouabah[2] and Wafa Feneniche[1]

[1]*ETA Laboratory, Electronics Department, University of Mohamed El Bachir EI-Ibrahimi. Bordj Bou Arreridj, Algeria*
[2]*Department of Electronics, Mohamed BOUDIAF University of M'sila, University Pole, Road Bordj Bou Arréridj, M'sila 28000 Algeria*

Received 16 July 2024; Accepted 13 October 2024

Abstract

In this paper, we present an enhanced modified multiplexed binary offset carrier (MMBOC) modulation method whose power spectral density (PSD) is defined in the same way as that of multiplexed binary offset carrier (MBOC). MMBOC results from multiplexing the Binary Offset Carrier BOC (1,1), BOC (6,1) and BOC (10,1) signals spectra, so that 1/11 power contribution of the BOC (6,1) signal in the PSD of MBOC signal will be distributed between BOC (6,1) and BOC (10,1) signals. This approach would supply the signal high frequency components, around ± 10 MHz, with higher power relative to the spectrum of the multiplexed binary offset carrier (MBOC) modulation. As a result, the autocorrelation functions (ACFs) of the MMBOC modulation implementation signals, namely, the modified composite BOC (MCBOC) and the modified time multiplexed BOC (MTMBOC) have a sharper central peak compared to those of the composite BOC (CBOC) and the time multiplexed BOC (TMBOC) signals, which gives a better limitation of multipath (MP) effects.

Keywords: BOC, MBOC, CBOC, TMBOC, GPS, Galileo, MMBOC, MCBOC, MTMBOC.

1. Introduction

The Global Positioning System (GPS) and the Galileo Working Group on Interoperability and Compatibility have recently approved the MBOC modulation at the L1 center frequency of 1575.42 MHz [1-2]. The PSD of the MBOC modulation is created by a linear combination of the BOC(1,1) and BOC(6,1) spectra. The contribution of BOC(6,1) in the PSD of MBOC increases the power on the higher frequencies of BOC(1,1) PSD in order to improve signal tracking performance [3-7]. Two different signals are used to implement the MBOC modulation with pilot and data channels, namely, the TMBOC for GPS L1C and the CBOC for Galileo OS L1 [1-2, 8-9]. The CBOC signal is based on the approach of the binary coded symbol (BCS) modulation [10-12] and composite binary coded symbols (CBCS) signal [13] expressed as a result of the weighted superposition of BOC(1,1) and BOC(6,1) signals on both data and pilot in order to generate also a MBOC spectrum [1-2, 8-9]. The TMBOC signal, that is a time multiplex of BOC(1,1) and BOC(6,1) signals, is applied to different chips of the spreading code on both data and pilot channels to produce an MBOC spectrum [1-2].

Several studies were launched to analyze and investigate the performance of the MBOC modulation in terms of MP mitigation [1-2, 8-9, 14-17] or interference suppression [1-2, 18-19]. All these studies confirm clearly the efficiency and superiority of MBOC modulation compared to BOC modulation.

In the recent years, various studies propose improvements to BOC modulations, such as the adoption of double binary offset carrier (DBOC) modulation, in order to enhance tracking accuracy. This proposal involves the utilization of a second stage waveform subcarrier, which is characterized by an increased number of high-frequency components as well as ACF peaks [20]. However, it has been observed that this approach results in a higher number of zero-crossing points, leading to tracking ambiguity and a subsequent decline in tracking accuracy. To address this issue, a new concept known as binary offset carrier modulation with adjustable width (BOC-AW) was introduced, featuring the adjustment of the width of three-level subcarrier waveforms {-1, 0, 1}. This innovative modulation scheme aims at mitigating MP effects and enhancing resistance to jamming [21]. It is important to note that irregular ACFs associated with this modulation may introduce instability in tracking. Nevertheless, the generalized binary offset carrier (GBOC) modulation offers a solution by utilizing generalized two-level waveforms {-1, 1} with variable dwell time factors to ensure robust MP mitigation [22]. Despite its advantages, The GBOC modulation shows a drawback of a poor compatibility observed with GPS L1C/A.

In an effort to address issues related to compatibility, the faded harmonics binary offset carrier (FH-BOC) modulation has been developed. This modulation strategy involves the creation of a new multi-level shape waveform by subtracting a quasi-square waveform from a BOC square waveform, even though this sacrifice may affect the performance of code-tracking and MP mitigation [23]. Moreover, to achieve higher spectral efficiency, continuous phase modulations (CPMs) have been under investigation for use in inter-satellite links [24-25], despite the higher complexity that they introduce to the receiver. Furthermore, an enhanced scheme has been proposed which involves dynamic adjusting modulation symbols based on the code chip period, offering a different approach for performance improvement.

In order to strike a balance between the receiver performance, tracking stability and compatibility, the subcarrier periodic shifting BOC (SPS-BOC) modulation has been introduced. This innovative modulation technique has been introduced by periodically modifying the subcarrier phase based on the spreading code chip period, resulting in an increased dynamic presence of high-frequency components

*E-mail address: mustapha.flissi@univ-bba.dz
ISSN: 1791-2377
doi:10.25103/jestr.175.17

[26]. The SPS-BOC modulation represents a flexible and improved approach derived from BOC modulations. Given the superior performance and simplified ACF exhibited by the low-order SPS-BOC modulation, there is potential to enhance overall performance by reconstructing MBOC signal using SPS-BOC as the low-order component. In [27], an improved multiplexed binary offset carrier modulation based on periodic offset subcarrier (MBOC-POS) has been introduced. In this approach, the lower-order component used is the SPS-BOC modulation instead of sine BOC modulation.

In this paper, an enhanced MMBOC modulation is presented. The MMBOC techniques involve methods like the unambiguous correlation functions to optimize signal design for global navigation satellite systems (GNSS) [28], constant-envelope multiplexing [29] and subcarrier periodic shifting [27]. These advancements aim to increase tracking accuracy, reduce false-locking and improve MP mitigation capabilities. By combining elements from different modulation schemes MMBOC provides higher performance and flexibility, which makes it a promising solution for next-generation satellite navigation signals design. The MMBOC modulation is the result of multiplexing the spectrum of the BOC(1,1), BOC (6,1) and BOC (10,1) signals. The BOC(10,1) spectrum is added to the MBOC spectrum in order to place more high frequency components in the resulting proposed MMBOC modulated signal. As a consequence, the MMBOC discrimination function would present a greater slope, which improves its MP mitigation performance.

Afterwards, we propose two different signals to implement the MMBOC modulation with pilot and data channels, namely, the modified composite BOC (MCBOC) and the modified time multiplexed BOC (MTMBOC). The ACFs of these implementation signals have a sharper central peak compared to those of the CBOC and TMBOC signals. The resultant PSD of the proposed MMBOC modulation is introduced. The Spectral Separation Coefficient (SSC), the Cramér Rao Lower Bound (CRLB) on code-tracking accuracy, the Root Mean Square Bandwidth (RMSB) and the Root Mean Square Error (RMSE) are also calculated. According to the results of SSC, CRLB, RMSB and RMSE, the suggested MMBOC modulation was shown to be effective in terms of noise resistance and interference separation using a front-end bandwidth of 24 MHz. Furthermore, the simulation results revealed that the proposed MMBOC modulation outperforms the MBOC modulation used by Galileo and GPS upgrades in terms of MP mitigation.

2. MBOC Modulation

By considering both channels' data and pilot, the $\mathbf{MBOC(6,1,1/11)}$ signal was defined based on its PSD given by [3-4]:

$$G_{MBOC\left(6,1,\frac{1}{11}\right)}(f) = \frac{10}{11} G_{BOC(1,1)}(f) + \frac{1}{11} G_{BOC(6,1)}(f) \quad (1)$$

Where $\mathbf{G_{BOC(p,q)}}$ is the normalized PSD of $\boldsymbol{BOC(p,q)}$ signals, given by [5-7]:

$$G_{BOC(p,q)}(f) = f_c \left(\frac{\sin\left(\frac{\pi f}{n f_c}\right) \sin\left(\frac{\pi f}{f_c}\right)}{\pi f \cos\left(\frac{\pi f}{n f_c}\right)} \right)^2 \quad (2)$$

In the above equation, $n = 2f_s/f_c = 2p/q$ is the number of half-periods T_s of the subcarrier in a code chip of duration T_c, as a result of which the ratio can be even or odd. $f_s = p \times f_0$ is the subcarrier frequency, $f_c = q \times f_0$ is the C/A spreading code frequency and $f_0 = 1.203\ MHz$: is the reference frequency of GPS.

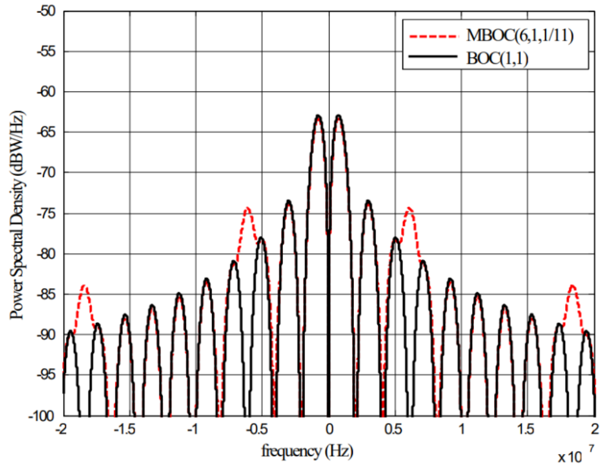

Fig. 1. Normalized PSDs of MBOC and BOC

Figure 1 shows the PSDs of the $\boldsymbol{MBOC(6,1,1/11)}$ and the $\boldsymbol{BOC(1,1)}$ signals. From the graph of the MBOC signal PSD, there is a considerable increase in power at frequencies of approximately ± 6 MHz relative to the $\boldsymbol{BOC(1,1)}$ spectrum. Two different approaches to achieve the implementation of the MBOC modulation have been proposed, namely $\boldsymbol{TMBOC(6,1,4/33)}$ for GPS L1C and $\boldsymbol{CBOC(6,1,1/11)}$ for the Galileo system E1 OS. These two approaches are temporal forms that produce the same spectrum of MBOC [1-2, 8-9].

3. MMBOC Concept

To further improve the performance of the MBOC modulation, another component of type $\boldsymbol{BOC(10,1)}$ is added to the MBOC spectrum so that the 1/11 power portion of $\boldsymbol{BOC(6,1)}$ is distributed between $\boldsymbol{BOC(6,1)}$ and $\boldsymbol{BOC(10,1)}$, in order to have higher power frequency components around ± 10 MHz, relative to the MBOC spectrum.

This proposed novel modulation scheme is denoted by $\boldsymbol{MMBOC(10,6,1,a/11,b/11)}$, where $\boldsymbol{a}$ and $\boldsymbol{b}$ denote, respectively, the power portion of the $\boldsymbol{BOC(10,1)}$ and $\boldsymbol{BOC(6,1)}$ relative to 1/11.

Then, the PSD of the $\boldsymbol{MMBOC(10,6,1,a/11,b/11)}$ can be written as follows:

$$G_{MMBOC}(f) = \frac{10}{11} G_{BOC(1,1)}(f) + \frac{a}{11} G_{BOC(10,1)}(f) + \frac{b}{11} G_{BOC(6,1)}(f) \quad (3)$$

Equation (3) may also be written as:

$$G_{MMBOC}(f) = \frac{f_c}{11\pi^2 f^2} \sin^2\left(\frac{\pi f}{f_c}\right) \left[10\tan^2\left(\frac{\pi f}{2f_c}\right) + a.\tan^2\left(\frac{\pi f}{20 f_c}\right) + b.\tan^2\left(\frac{\pi f}{12 f_c}\right)\right] \quad (4)$$

The choice of $\boldsymbol{a}$ and $\boldsymbol{b}$ is not arbitrary because of the size of the PRN code that is 10230 for GPS and 4092 for Galileo. That is to say, we must look for a number among the common divisors (CD) between 4092 and 10230 {i.e. 2, 3, 6, 11, 22, 31, 33, 62, 93, 186, 341, 682, 1023, 2046} that represents the common multiplier (CM) between 11 ($\boldsymbol{CBOC(6,1,1/11)}$) and 33 ($\boldsymbol{TMBOC(6,1,4/33)}$). Once found the valuesof $\boldsymbol{a}$ and $\boldsymbol{b}$ are defined as the fractions of that number. Thus, we must solve the following system of equations:

$$\begin{cases} \mathbf{11}\boldsymbol{X} = \boldsymbol{Y} & \boldsymbol{Y} \in \boldsymbol{CD}(\mathbf{10230}, \mathbf{4092}) \\ \mathbf{33}\boldsymbol{X} = \boldsymbol{Z} & \boldsymbol{Z} \in \boldsymbol{CD}(\mathbf{10230}, \mathbf{4092}) \end{cases} \tag{5}$$

The solution of (5) is $\boldsymbol{X} = \mathbf{62}$.

We can thus choose: $\boldsymbol{a} = \mathbf{13/62}$ and $\boldsymbol{b} = \mathbf{49/62}$.

Figure 2 shows the PSD of $\boldsymbol{MMBOC(10,6,1,13/682,49/682)}$, $\boldsymbol{MBOC(6,1,1/11)}$ and $\boldsymbol{BOC(1,1)}$signals. From the shape of the MMBOC signal PSD, there is a considerable increase in power at frequencies of approximately ± 6 MHz and ± 10 MHz compared to the $\boldsymbol{BOC(1,1)}$ spectrum.

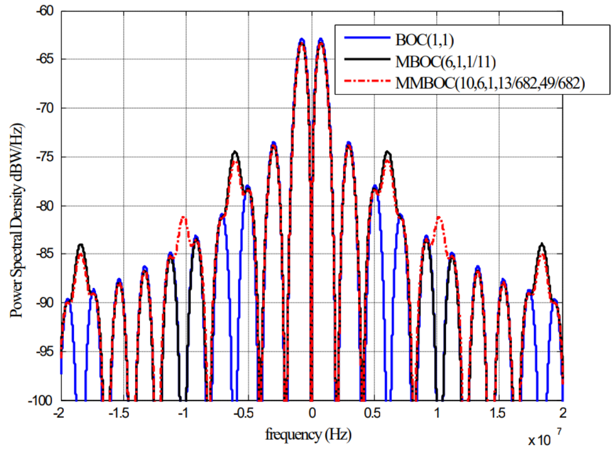

Fig. 2. Normalized PSDs of BOC, MBOC and MMBOC

4. MMBOC Implementation

In the following are proposed two different approaches for MMBOC implementation signals that are based on the same principles used in [3-4, 8-9, 13], namely the MTMBOC and MCBOC signals. Both implementations use BOC(10,1) signal in addition to BOC(1,1) and BOC(6,1) signals. Figures 3 and 4 show the graphs of MTMBOC and MCBOC signals, respectively.

Following the same reasoning given for CBOC in [13], the subcarrier of the MCBOC can be generated as follows:

$$\boldsymbol{s_{MCBOC}(t)} = \boldsymbol{\alpha s_{BOC(1,1)}(t)} + \boldsymbol{\beta s_{BOC(10,1)}(t)} + \boldsymbol{\gamma s_{BOC(6,1)}(t)} \tag{6}$$

Where $\boldsymbol{s_{BOC(1,1)}(t)}$, $\boldsymbol{s_{BOC(10,1)}(t)}$ and $\boldsymbol{s_{BOC(6,1)}(t)}$ are the BOC(1,1), BOC(10,1) and BOC(6,1) subcarriers respectively, and $\boldsymbol{\alpha}, \boldsymbol{\beta}$ and $\boldsymbol{\gamma}$ are some weighting factors such that :

$$\boldsymbol{\alpha}^2 + \boldsymbol{\beta}^2 + \boldsymbol{\gamma}^2 = \mathbf{1} \tag{7}$$

A block diagram corresponding to the equation (6) is shown in Figure (5).

The MTMBOC signal results from time-multiplexing the BOC(1,1), BOC(6,1) and BOC(10,1) signals. Similar to the reasoning given for TMBOC in [3-4], the signal duration is divided into blocks of $\boldsymbol{N}$ code symbols allocated among the BOC(1,1), BOC(10,1) and BOC(6,1) signals, with respective block sizes $\boldsymbol{N1}$, $\boldsymbol{N2}$ and $\boldsymbol{N3}$, such that $\boldsymbol{N2} < \boldsymbol{N3} < \boldsymbol{N1} < \boldsymbol{N}$. The choice of $\boldsymbol{N}$, $\boldsymbol{N1}$, $\boldsymbol{N2}$, and $\boldsymbol{N3}$ depends on the power distribution between pilot and data channels. Below, three possible configurations are proposed.

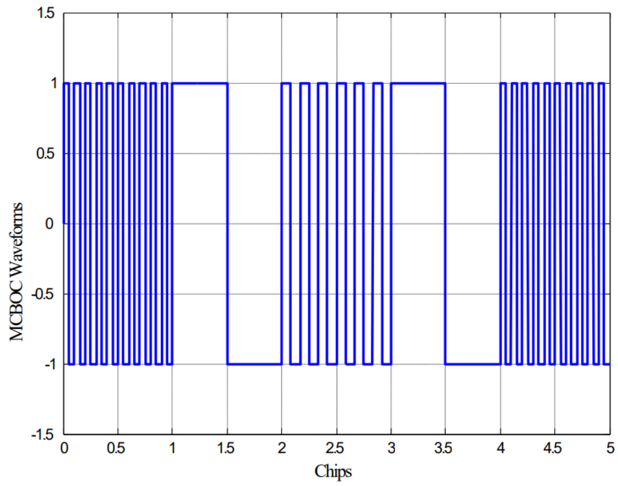

Fig. 3. MTMBOC modulated signal

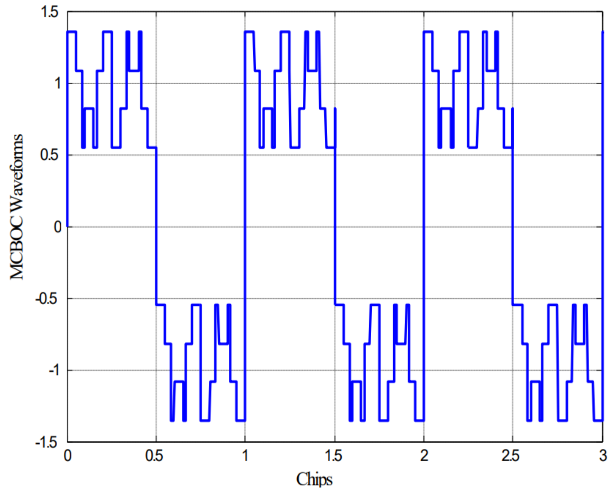

Fig. 4. MCBOC modulated signal

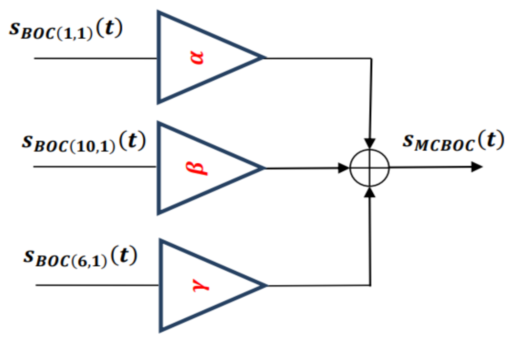

Fig. 5. Block diagram illustrating the generation of the MCBOC subcarrier

The MTMBOC signal results from time-multiplexing the BOC(1,1), BOC(6,1) and BOC(10,1) signals. Similar to the reasoning given for TMBOC in [3-4], the signal duration is divided into blocks of $\boldsymbol{N}$ code symbols allocated among the BOC(1,1), BOC(10,1) and BOC(6,1) signals, with respective block sizes $\boldsymbol{N1}$, $\boldsymbol{N2}$ and $\boldsymbol{N3}$, such that $\boldsymbol{N2} < \boldsymbol{N3} < \boldsymbol{N1} < \boldsymbol{N}$. The choice of $\boldsymbol{N}$, $\boldsymbol{N1}$, $\boldsymbol{N2}$, and $\boldsymbol{N3}$ depends on the power distribution between pilot and data channels. Below, three possible configurations are proposed.

4.1. First configuration

The $\boldsymbol{MTMBOC(10, 6, 1, 26/1023, 98/1023)}$ signal or the $\boldsymbol{MCBOC(10, 6, 1, 26/1023, 98/1023)}$ signal is used for the Pilot component and the $\boldsymbol{BOC(1, 1,)}$ signal is used for the Data component. The power distribution between the Data / Pilot components is 25% / 75%.

The PSDs of data, pilot and MMBOC signals are given as:

$$\boldsymbol{G_{Pilot}(f) = \frac{29}{33} G_{BOC(1,1)}(f) + \frac{13}{62}\frac{4}{33} G_{BOC(10,1)}(f) + \frac{49}{62}\frac{4}{33} G_{BOC(6,1)}(f) = \frac{899}{1023} G_{BOC(1,1)}(f) + \frac{26}{1023} G_{BOC(10,1)}(f) + \frac{98}{1023} G_{BOC(6,1)}(f)} \quad (8)$$

$$\boldsymbol{G_{Data}(f) = G_{BOC(1,1)}(f)} \quad (9)$$

$$\boldsymbol{G_{MMBOC}(f) = \frac{3}{4} G_{Pilot}(f) + \frac{1}{4} G_{Data}(f) = \frac{620}{682} G_{BOC(1,1)}(f) + \frac{13}{682} G_{BOC(10,1)}(f) + \frac{49}{682} G_{BOC(6,1)}(f)} \quad (10)$$

4.2. Second configuration

In this configuration, the $\boldsymbol{MTMBOC(10, 6, 1, 26/682, 98/682)}$ signal or the $\boldsymbol{MCBOC(10, 6, 1, 26/682, 98/682)}$ signal is used for the Pilot component and the $\boldsymbol{BOC(1, 1,)}$ signal is used for the Data component. The power distribution between the Data / Pilot components is 50% /50%. The PSDs of data, pilot and MMBOC signals are given as:

$$\boldsymbol{G_{Pilot}(f) = \frac{9}{11} G_{BOC(1,1)}(f) + \frac{13}{62}\frac{2}{11} G_{BOC(10,1)}(f) + \frac{49}{62}\frac{2}{11} G_{BOC(6,1)}(f) = \frac{558}{682} G_{BOC(1,1)}(f) + \frac{26}{682} G_{BOC(10,1)}(f) + \frac{98}{682} G_{BOC(6,1)}(f)} \quad (11)$$

$$\boldsymbol{G_{Data}(f) = G_{BOC(1,1)}(f)} \quad (12)$$

$$\boldsymbol{G_{MMBOC}(f) = \frac{1}{2} G_{Pilot}(f) + \frac{1}{2} G_{Data}(f) = \frac{620}{682} G_{BOC(1,1)}(f) + \frac{13}{682} G_{BOC(10,1)}(f) + \frac{49}{682} G_{BOC(6,1)}(f)} \quad (13)$$

4.3. Third configuration

Here, the $\boldsymbol{MTMBOC(10, 6, 1, 13/682, 49/682)}$ signal or the $\boldsymbol{MCBOC(10, 6, 1, 13/682, 49/682)}$ signal is used for both Data/Pilot components. The power distribution between the Data / Pilot components is 50% /50% or 25%/75%. The PSDs of data, pilot and MMBOC signals are given as:

$$\boldsymbol{G_{Pilot}(f) = \frac{10}{11} G_{BOC(1,1)}(f) + \frac{13}{62}\frac{1}{11} G_{BOC(10,1)}(f) + \frac{49}{62}\frac{1}{11} G_{BOC(6,1)}(f) = \frac{620}{682} G_{BOC(1,1)}(f) + \frac{13}{682} G_{BOC(10,1)}(f) + \frac{49}{682} G_{BOC(6,1)}(f)} \quad (14)$$

$$\boldsymbol{G_{Data}(f) = \frac{620}{682} G_{BOC(1,1)}(f) + \frac{13}{682} G_{BOC(10,1)}(f) + \frac{49}{682} G_{BOC(6,1)}(f)} \quad (15)$$

$$\boldsymbol{G_{MMBOC}(f) = \frac{1}{2} G_{Pilot}(f) + \frac{1}{2} G_{Data}(f) \text{ or } G_{MMBOC}(f) = \frac{3}{4} G_{Pilot}(f) + \frac{1}{4} G_{Data}(f)} \quad (16)$$

$$\boldsymbol{\frac{620}{682} G_{BOC(1,1)}(f) + \frac{13}{682} G_{BOC(10,1)}(f) + \frac{49}{682} G_{BOC(6,1)}(f)} \quad (17)$$

Table 1. Possible implementations of MMBOC(10, 6, 1, 13/682, 49/682)

Data	Pilot	Power proportion
MTMBOC(10, 6, 1,13/682, 49/682)	MTMBOC(10, 6, 1,13/682, 49/682)	75%
MTMBOC(10, 6, 1,13/682, 49/682	MTMBOC(10, 6, 1,13/682, 49/682)	50%
BOC(1,1)	MTMBOC(10, 6, 1, 26/1023, 98/1023)	75%
BOC(1,1)	MTMBOC(10, 6, 1, 26/1023, 98/1023)	50%
MCBOC(10, 6, 1,13/682, 49/682)	MCBOC(10, 6, 1,13/682, 49/682)	75%
MCBOC(10, 6, 1,13/682, 49/682)	MCBOC(10, 6, 1,13/682, 49/682)	50%
BOC(1,1)	MCBOC(10, 6, 1, 26/1023, 98/1023)	75%
BOC(1,1)	MCBOC(10, 6, 1, 26/1023, 98/1023)	50%

In the Table 1, the possible implementations of $\boldsymbol{MMBOC(10, 6, 1, 13/682, 49/682)}$ are given for different distributions of Data / Pilot power.

We show in figures 6, 7, 8, 9 and 10, the ACFs of the different concepts of MTMBOC and MCBOC signals compared with those of the TMBOC, CBOC and BOC(1,1) signals.

It is clear from these figures that the ACFs of MTMBOC and MCBOC are narrower than those of TMBOC and CBOC. Consequently, the performance of code tracking will be improved.

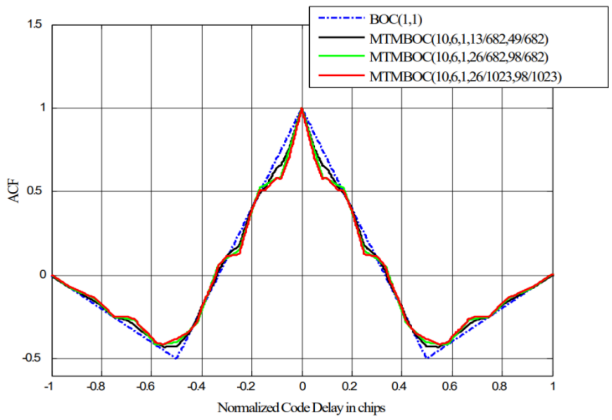

Fig. 6. Normalized ACFs of BOC(1, 1), MTMBOC(10, 6, 1, 13/682,49/682), MTMBOC(10, 6, 1, 26/682,98/682) and MTMBOC(10, 6, 1, 26/1023, 98/1023)

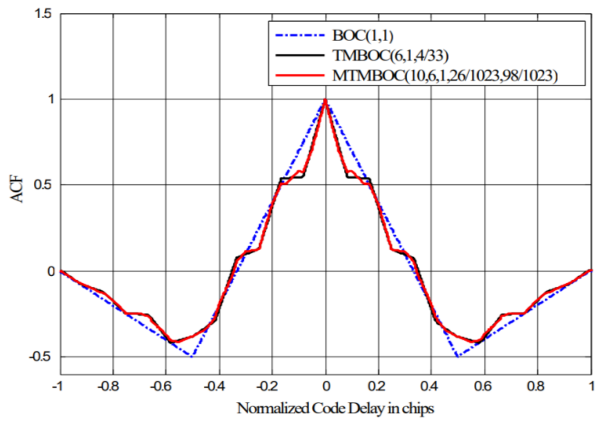

Fig. 7. Normalized ACFs of BOC(1, 1), TMBOC(6, 1,4/33), and MTMBOC(10, 6, 1, 26/1023, 98/1023.

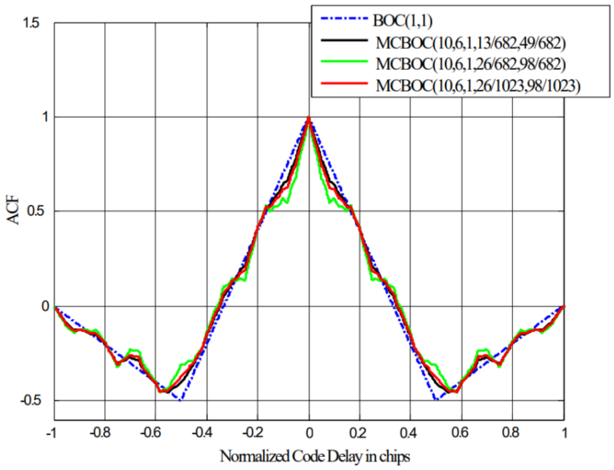

Fig. 8. Normalized ACFs of BOC(1, 1), MCBOC(10, 6, 1, 13/682,49/682), MCBOC(10, 6, 1, 26/682,98/682), and MCBOC(10, 6, 1, 26/1023, 98/1023).

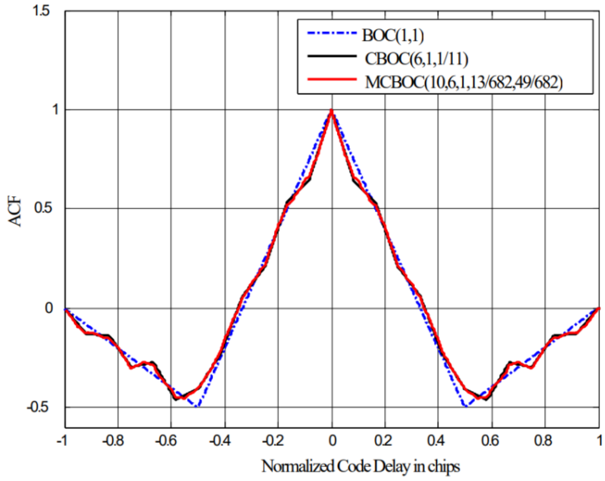

Fig. 9. Normalized ACFs of BOC(1, 1), CBOC(6, 1,1/11), and MCBOC(10, 6, 1, 13/682, 49/682)

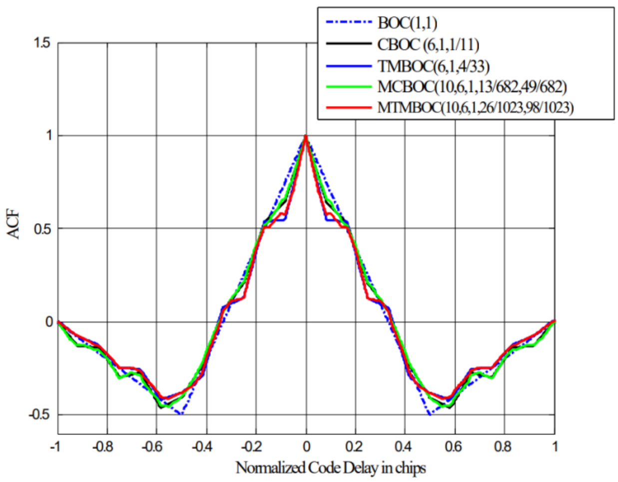

Fig. 10. Normalized ACFs of BOC(1, 1), CBOC(6, 1, 1/11) ,TMBOC(6, 1, 4/33), MCBOC(10, 6, 1, 13/682, 49/682) and MTMBOC(10, 6, 1, 26/1023, 98/1023).

5. MMBOC Performance Evaluation

5.1. Code-Tracking Accuracy and RMS Bandwidth

Two criteria are used to evaluate the code tracking accuracy (i.e; the noise effect) of the proposed MMBOC modulation. The first one is the CRLB, denoted by σ_{LB}, which is the RMSE or any non-random parameter estimate and is given by [7][30][31]:

$$\sigma_{LB} = \frac{1}{2\pi\beta_{RMS}}\sqrt{\frac{B_L}{\lambda\frac{C}{N_0}}} \qquad (18)$$

Where, B_L is the loop bandwidth of the code tracking loop, C/N_0 is the carrier-power-to-noise-density ratio, and λ is the correlation loss due to front-end bandwidth B_r defined as:

$$\lambda = \int_{-B_r/2}^{B_r/2} G_s(f)df \qquad (19)$$

and

β_{RMS} : is the Root Mean Square Bandwidth (RMSB)and represents the second criterion. It is defined as:

$$\beta_{RMS} = \left(\int_{-B_r/2}^{B_r/2} f^2\bar{G}_s(f)df\right)^{1/2} \qquad (20)$$

Where $\bar{G}_s(f)$ is the signal PSD normalized for unit power over the front-end bandwidth B_r.

We offer these curves in order to understand how the code tracking noise acts for the set of modulations studied in this paper.Figures 11, 12 and 13 show the CRLB (or RMS Code Tracking Errors) using a 24 MHz front-end bandwidth.

As we can notice from these figures, the MCBOC(10,6,1,13/682,49/682) and MTMBOC(10,6,1,26/1023, 98/1023) modulations give significantly higher code-tracking precision than CBOC(6,1,1/11), TMBOC(6,1,4/33). In addition, MTMBOC(10,6,1,26/1023,98/1023) modulations provide much better code-tracking accuracy than BOC(2,2). However, BOC(2,2) modulation has better code-tracking accuracy than MCBOC(10, 6,1,13/682,49/682) modulation.

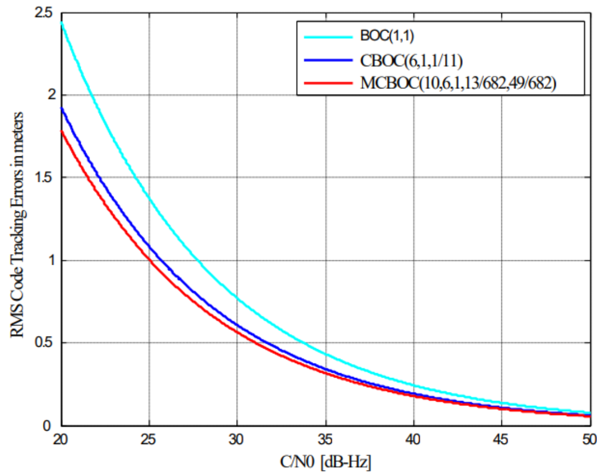

Fig. 11. RMS Code Tracking Errors of BOC(1, 1), CBOC(6, 1, 1/11) and MCBOC(10, 6, 1, 13/682, 49/682) with 24 MHz front-end bandwidth.

In figures (14), (15) and (16) the RMSB criterion is used giving a comparative study between the proposed MMBOC signals, their counterpart MBOC signals and a couple of classical BOC(n,n) signals.

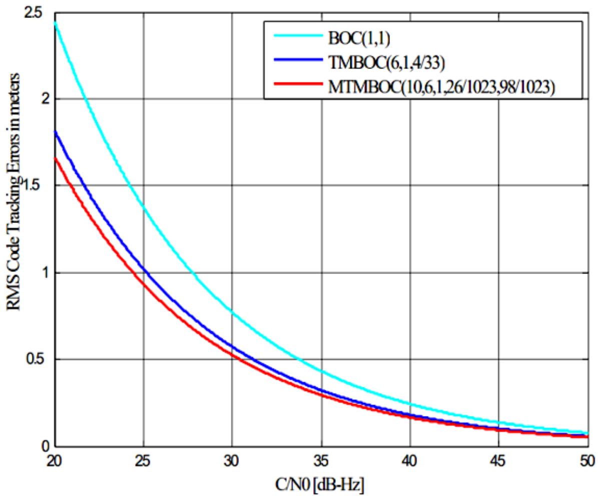

Fig. 12. RMS Code Tracking Errors of BOC(1, 1), TMBOC(6, 1, 4/33) and MTMBOC(10, 6, 1, 26/1023, 98/1023) with 24 MHz front-end bandwidth

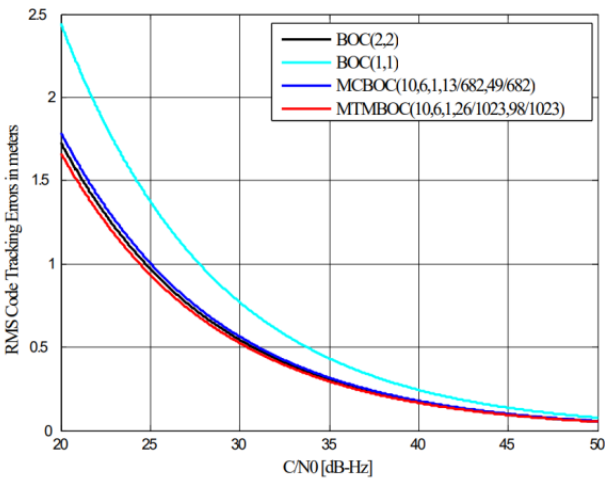

Fig. 13. RMS Code Tracking Errors of BOC(1, 1), BOC(2, 2), MCBOC(10, 6, 1, 13/682, 49/682) and MTMBOC(10, 6, 1, 26/1023, 98/1023) with 24 MHz front-end bandwidth.

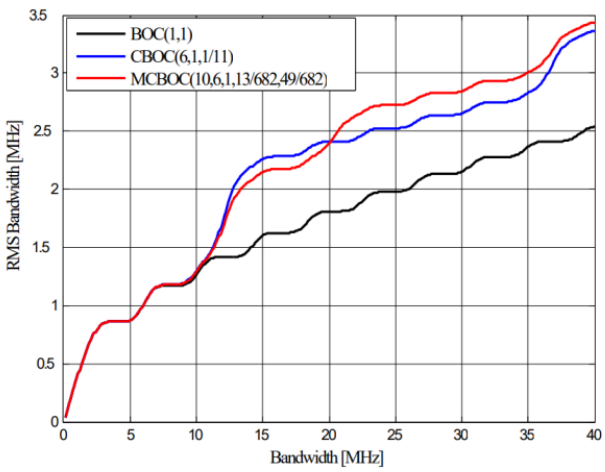

Fig. 14. RMSB of BOC(1, 1), CBOC(6, 1, 1/11) and MCBOC(10, 6, 1, 13/682, 49/682).

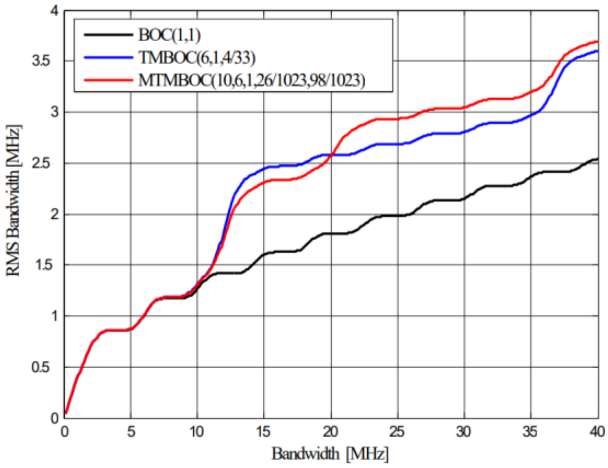

Fig. 15. RMSB of BOC(1, 1), TMBOC(6, 1, 4/33) and MTMBOC(10, 6, 1, 26/1023, 98/1023).

Figures 14 and 15, show, on the one hand, the absolute superiority of MCBOC (10,6,1,13/682,49/682) and MTMBOC(10,6,1,26/1023, 98/1023) over BOC(1,1). On the other hand, these same figures illustrate that MCBOC (10,6,1,13/682,49/682) and MTMBOC(10,6,1,26/1023,98/1023) signals have RMSB values that are greater than those of CBOC(6,1,1/11) and TMBOC(6,1,4/33), respectively, for receiver bandwidth superior to 20 MHz, which makes them more efficient in this range.

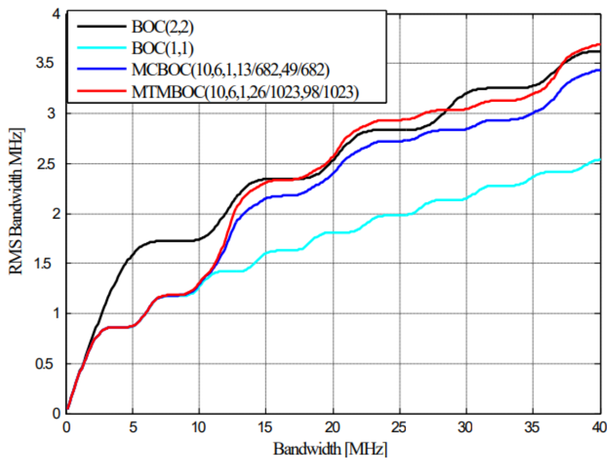

Fig. 16. RMSB of BOC(1, 1), BOC(2, 2), MCBOC(10, 6, 1, 13/682, 49/682) and MTMBOC(10, 6, 1, 26/1023, 98/1023).

Figure 16 shows that for receiver bandwidth less than 12 MHz the MCBOC(10,6,1,13/682,49/682) and MTMBOC(10,6,1,26/1023,98/1023) signals present the same RMSB values. However, for bandwidths greater than 12 MHz the RMSB of MTMBOC(10,6,1,26/1023,98/1023) is the highest, which qualifies this latter to have better performance in this range. Besides, this same figure, exhibits the performance superiority of BOC(2,2) within the receiver bandwidth interval from 3 MHz to 18 MHz.

5.2. Spectral separation coefficient

The SSC between desired signal and interfering signal can be expressed in terms of the receiver front end filter bandwidth $\boldsymbol{B_r}$ and the normalized PSDs $\boldsymbol{G_i(f)}$ and $\boldsymbol{G_s(f)}$ of the interfering signal and desired signal, respectively [32-34]:

$$k_{is} = \int_{-B_r/2}^{B_r/2} G_s(f)G_i(f)df \quad (21)$$

In tables 2 and 3, several SSC results are given respectively for the cases of the 30,69 MHz and 40,92 MHz transmission bandwidths and a 24MHz single receiver bandwidth.

Table 2. SSCs [dB] between the BOC(1,1), MBOC(6,1,1/11), MMBOC(10, 6, 1, 13/682, 49/682) signals and the GPS signals for a 30,69 MHz transmission bandwidth and a 24MHz single receiver bandwidth.

Signals	SSC		
	BOC(1,1)	MBOC	MMBOC
GPS P(Y) Code BPSK(10)	-70.0984	-70.4118	-70.4310
GPS C/A Code BPSK(1)	-67.8509	-68.2528	-68.2544
GPS BOC(1,1)	-64.7812	-65.1891	-65.1899
GPS M Code BOC(10,5)	-82.3571	-82.1000	-81.3208
GPS L1C MBOC	-65.1236	-65.5028	-65.5096
GPS MMBOC	-65.1241	-65.5092	-65.5135

Table 3. SSCs [dB] between the BOC(1,1), MBOC(6,1,1/11), MMBOC(10, 6, 1, 13/682, 49/682) signals and the Galileo signals for a 40,92 MHz transmission bandwidth and a 24MHz single receiver bandwidth.

Signals	SSC		
	BOC(1,1)	MBOC	MMBOC
Galileo BOC(1,1)	-64.8037	-65.2116	-65.2124
Galileo E1 PRS BOCc(15,2.5)	-103.2716	-101.5806	-101.3478
Galileo E1 OS MBOC	-65.1792	-65.5583	-65.5651
Galileo MMBOC	-65.1724	-65.5575	-65.5618

As we can recognize from these tables, similar to the MBOC signal, the MMBOC one presents a better SSC with the GNSS signals E1/L1. For example, the SSC for MMBOC signal with GPS C/A code is 0.33dB higher than the BOC(1,1) utilizing the same code and is 0.02dB higher than the MBOC. Also, the SSCs for MMBOC with GPS P(Y) code is 0.33dB higher than BOC(1,1) and is 0.02dB higher than MBOC with the same code. However, the SSC for MBOC signal presents better spectral separation with GPS M code and Galileo E1 PRS compared with MMBOC.

5.3. Experimental results

The simulation process follows the following steps:

Step 1: In this step, we generate the BOC (1,1), TMBOC, and the proposed MTMBOC signals using MATLAB, ensuring accurate spectral shaping according to the specified modulation parameters (See Figure (3) for our proposed MCBOC signal).
Step 2: In this step, the signals are then transmitted through a simulated channel, which includes noise and single MP signal (See Figure (17)).
Step 3: In this step, we vary MP delay to evaluate the signal performance, calculating the RAE.
Step 4: In this step, we introduce varying Signal to Noise Ratio (SNR) levels to evaluate the signal performance, calculating the RMSE for each signal across different conditions.
Step 5: In this step, the performance of each signal is then analyzed in terms of RMSE and RAE. In addition, the results are compared to identify which modulation method offers superior performance.

5.4. Multipath and noise performance

In order to show the performance of the proposed MMBOC Modulation in the presence of MP signals, simulations were carried out using an MP channel with a single reflected signal and a line-of-sight (LOS) signal as shown in figure 17.

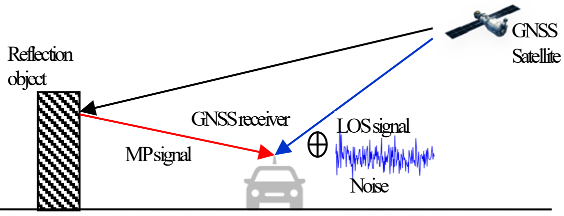

Fig. 17. MP phenomenon

After passing through the intermediate frequency stage, the received signal from a single GNSS satellite, affected by one MP signal and noise, can be expressed as follows [35] :

$$s_r(t) = Re\left(\sum_{l=0}^{1} a_l C_{fil}(t-\tau_l) D_{fil}(t-\tau_l) \cdot \exp\left(j(2\pi(f_{IF} + f_D)t + \varphi_l)\right) + n(t)\right) \quad (22)$$

Where:
τ_l: LOS or MP signal delay;
φ_l : LOS or MP signal phase;
f_{IF}: Intermediate frequency;
f_D : Doppler frequency;
a_l : LOS or MP signal coefficient amplitude;
$n(t)$: Narrow band noise;
$C_{fil}(t)$: Filtered PRN code and subcarrier;
$D_{fil}(t)$: Filtered navigation data.

In our experiment, based on the mathematical model given by (22), the MP signal has 0.5 amplitude and a delay ranging from 0 to 450 m relative to the LOS delay [21, 36]. The MP error envelopes, calculated by determining the zero-crossing point of the delay locked loop (DLL) discriminator (illustrated in Figure 18), are used to compute the running average errors (RAE) for 24 MHz pre-correlation bandwidth.

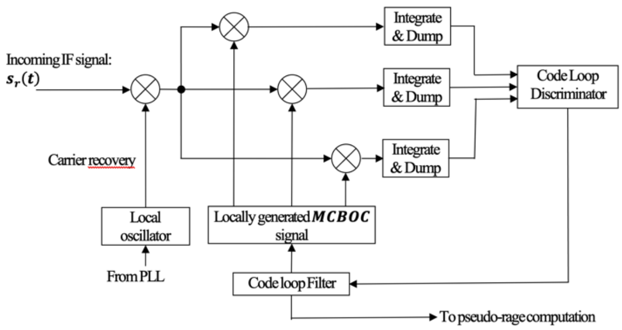

Fig. 18. DLL loop used to track all signals.

The RAE curves for TMBOC(6,1,4/33), MTMBOC(10,6,1,26/1023,98/1023) and BOC(1,1) signals, as presented in Figure 19, show that the proposed MTMBOC(10,6,1,26/1023,98/1023) signal displays the best performance in terms of RAE for all the band of variation of the MP delay as compared to TMBOC(6,1,4/33) and BOC(1,1) signals.
Figure 20 presents the RAE curves for MCBOC(10,6,1,13/682, 49/682), CBOC(6,1,1/11) and BOC(1,1) signals. It can be seen clearly from this figure that the proposed MCBOC(10,6,1,13/682,49/682) signal

performs better than the CBOC(6,1,1/11) and BOC(1,1) signals.

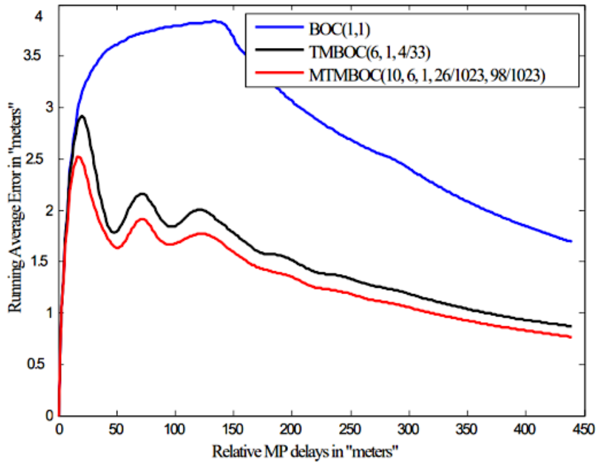

Fig. 19. RAEs of BOC(1, 1), TMBOC(6, 1, 4/33) and MTMBOC(10, 6, 1, 26/1023, 98/1023).

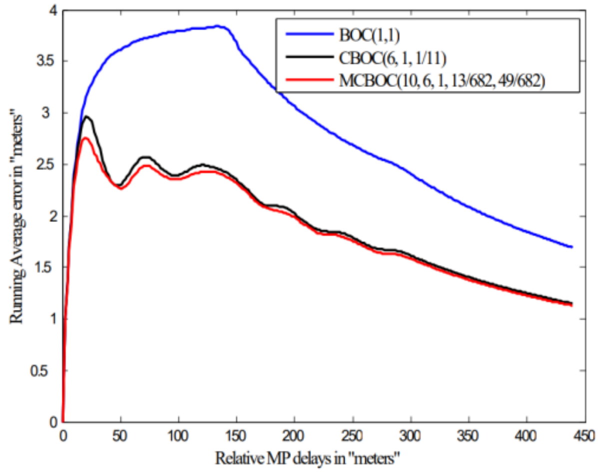

Fig. 20. RAEs of BOC(1, 1), CBOC(6, 1, 1/11) and MCBOC(10, 6, 1, 13/682, 49/682).

To facilitate the comparative study, the results of the RAE of BOC(2,2), BOC(1,1) signals, along with the proposed MTMBOC(10,6,1,26/1023,98/1023) and MCBOC(10,6,1,13/682,49/682) signals, are illustrated together in Figure 21. As shown in this figure, the MTMBOC(10,6,1,26/1023,98/1023) signal shows the best performance for all MP delays less than approximately 340 m. Beyond this value, the best performance is given by the BOC(2,2) signal. However, the MCBOC(10,6,1,13/682,49/682) signal presents a better performance relative to BOC(1,1) and BOC(2,2) signals only for delays less than 110 m, and BOC(1,1) presents the worst case for all MP delays.

It can be seen from figure 22 that the proposed MTMBOC(10,6,1,26/1023,98/1023) signal clearly achieves the best performance than the TMBOC(6,1,4/33) and BOC(1,1) signals regardless of the SNR value. In figure 23, it can be seen that the MCBOC(10,6,1,13/682,49/682) and CBOC(6,1,1/11) signals show almost the same performance for SNR values approximately greater than -28dB, while MCBOC(10,6,1,13/682,49/682) performs better for SNR values below -28dB.

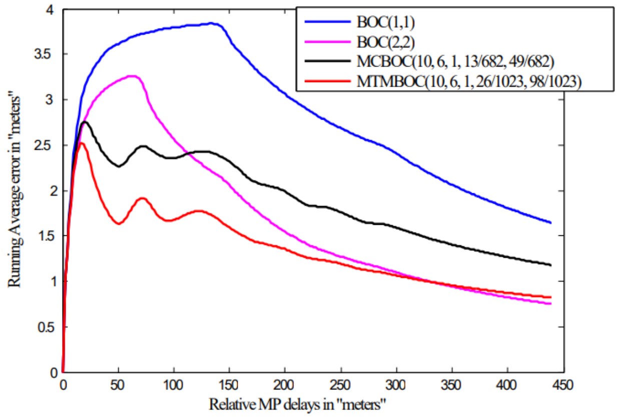

Fig. 21. RAEs of BOC(1, 1), BOC(2, 2), MCBOC(10, 6, 1, 13/682, 49/682) and MTMBOC(10, 6, 1, 26/1023, 98/1023)

To complete this section, the RMSEs of code tracking are plotted in meters in function of SNR, which ranges from −35 to −20 dB. The results are shown in the figures 22 and 23.

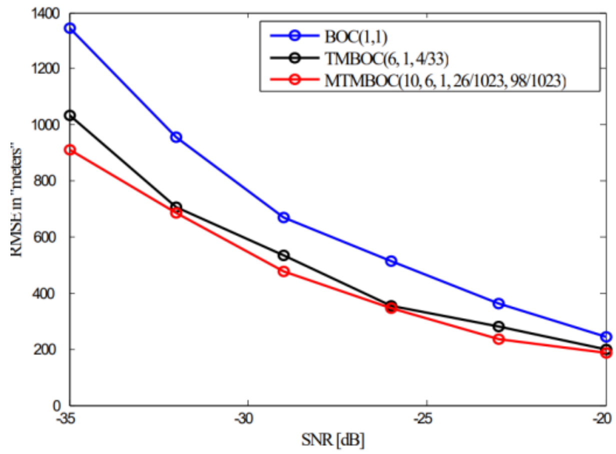

Fig. 22. RMSEs of BOC(1, 1), TMBOC(6, 1, 4/33) and MTMBOC(10, 6, 1, 26/1023, 98/1023).

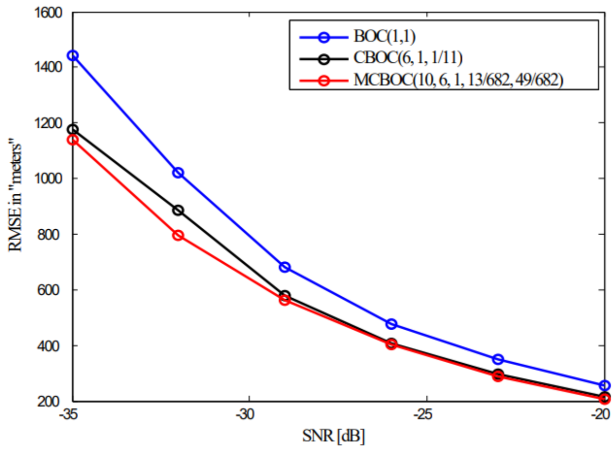

Fig. 23. RMSEs of BOC(1, 1), CBOC(6, 1, 1/11) and MCBOC(10, 6, 1, 13/682, 49/682).

6. Conclusions

In this paper, an enhanced MMBOC modulation, based on multiplexing the spectra of the BOC(1,1), BOC(6,1) and BOC(10,1) signals with different power levels, is proposed. Two implementation signals, namely MTMBOC and MCBOC, for MMBOC modulation, were presented and compared with the existing TMBOC and CBOC modulated signals. The MTMBOC(10,6,1,26/1023,98/1023) signal has shown the best performance in terms of MP mitigation due to its ACF characteristics. In addition, our study showed that the proposed MMBOC modulation, with its distributed DSP approach, presents better resistance against noise and interference compared to the traditional MBOC modulation. Finally, further research is needed to find a modified version of interplex modulation grouping the implementation signals of the proposed MMBOC modulation.

References

[1] GJU, "Galileo joint undertaking - GPS-Galileo Working Group A (WGA) Recommendations on L1 OS/LIC optimization," Mar. 2006. [Online]. Available: https://www.gps.gov/policy/cooperation/europe/2006/joint-statement/

[2] X. Zhao, X. Huang, Z. Liu, Z. Xiao, and G. Sun, "Improved MBOC modulations based on periodic offset subcarrier," *IET Commun.*, vol. 15, no. 14, pp. 1831-1848, Jul. 2021.

[3] G. W. Hein, J. A. Avila-Rodriguez, S. Wallner, A. R. Pratt, J. Owen, J. L. Issler, *et al*., "MBOC: The new optimized spreading modulation recommended for GALILEO L1 OS and GPS L1C," in *Proc. IEEE/ION PLANS 2006*, Apr. 2006, pp. 883-892.

[4] J. Ma, Y. Yang, H. Li, J. Li, "Expressions for the autocorrelation function and power spectral density of BOC modulation based on convolution operation," *Math. Probl. in Eng.*, vol. 2020, pp. 1-12, Jun. 2020.

[5] J. W. Betz, "Binary offset carrier modulations for radionavigation," *J. Inst. Navig.*, vol. 48, pp. 227-246, Winter 2001-2002.

[6] K. Rouabah, S. Atia, M. Flissi, M. Salim Bouhlel, and S. Mezaache, "Efficient technique for DLL S-curve side zero-crossings cancellation in global positioning system/Galileo receiver," *IET Signal Process.*, vol. 13, no. 3, pp. 338-347, May 2019.

[7] A. Emmanuele, *Signal design and theoretical bounds for time-of-arrival estimation in GNSS applications*, PhD Thesis, di Pisa Univ., Pisa, Italy, 2012.

[8] J. A. Avila-Rodriguez, S. Wallner, G. Hein, E. Rebeyrol, O. Julien, C. Macabiau, *et al*., "CBOC: An implementation of MBOC," in *Proc. CNES-ESA*, *1st Workshop on GALILEO Signals and Signal Process.*, Oct. 2006.

[9] D. Arora and P. Patidar, "Analysis of Correlation Loss for MBOC Signals," in *Proc. 36th Int. Tech. Meeting Satellite Div. Inst. Nav. (ION GNSS+ 2023)*, Sep. 2023, pp. 3499-3512.

[10] M. Flissi, K. Rouabah, S. Attia, D. Chikouche, and T. Devers, "Consistent BCS modulated signals for GNSS applications," *IET Signal Process.*, vol. 11, no. 4, pp. 415-421, Jun. 2017.

[11] C. Hegarty, J. W. Betz, and A. Saidi, "Binary coded symbol modulations for GNSS," in *Proc. 60th Ann. Meeting Inst. Navig.*, Jun. 2004, pp. 56-64.

[12] Z. Yao and M. Lu, *Next-Generation GNSS Signal Design*, pp. 89-162, Singapore: Springer, 2021.

[13] G. W. Hein, J. A. Avila-Rodriguez, L. Ries, L. Lestarquit, J. L. Issler, J. Godet, and T. Pratt, "A candidate for the Galileo L1 OS optimized signal," in *Proc. 18th Int. Tech. Meeting Satellite Div. Inst. Navig. (ION GNSS 2005)*, Sept. 2005, pp. 833-845.

[14] E. S. Lohan and M. Renfors, "Correlation properties of multiplexed-BOC (MBOC) modulation for future GNSS signals," in *Eur. Wireless Conf.*, France, Apr. 2007.

[15] M. Fantino, P. Mulassano, F. Dovis, and L. Lo Presti, "Performance of the proposed Galileo CBOC modulation in heavy multipath environment," *Wireless Pers. Commun.*, vol. 44, pp. 323-339, Oct. 2008.

[16] F. Dovis, L. Lo Presti, M. Fantino, P. Mulassano, and J. Godet, "Comparison between Galileo CBOC candidates and BOC (1, 1) in terms of detection performance," *Int. J. Navig. Observ.*, vol. 2008, pp. 1-9, Apr. 2008.

[17] N. Hoult, E. Aguado, and P. Xia, "MBOC and BOC (1,1) performance comparison," *J. Navig.*, vol. 61, pp. 613-627, Oct. 2008.

[18] S. Wallner, G. W. Hein, and J. A. Avila-Rodriguez, "Interference computations between several GNSS systems," in *proc. ESA Navitec 2006*, Noordwijk, The Netherlands, Dec. 2006, pp 1-10.

[19] Y. Ran, X. Hu, T. Ke, and Y. Liu, "Interference analysis of interplex modulation in GALILEO E1 band," in *2009 5th Int. Conf. Wireless Commun., Netw. Mobile Comput.*, Sep. 2009, pp. 1-4.

[20] E. S. Lohan, A. Lakhzouri, and M. Renfors, "Binary-offset-carrier modulation techniques with applications in satellite navigation systems," *Wireless Commun. Mobile Comput.*, vol. 7, no. 6, pp. 767-779, Jul. 2007.

[21] W. Liu, Y. Hu, and X. Q. Zhan, "Generalised binary offset carrier modulations for global navigation satellite systems," *Electron. Lett.*, vol. 48, no. 5, pp. 284-286, Mar. 2012.

[22] W. Liu and Y. Hu, "Cosine faded harmonics binary offset carrier modulation for next-generation GNSS," *Electron. Lett.*, vol. 52, no. 1, pp. 68-70, Jan. 2016.

[23] R. Xue, H. Yu, and Q. Cheng, "Adaptive coded modulation based on continuous phase modulation for inter-satellite links of global navigation satellite systems," *IEEE Access*, vol. 6, pp. 20652-20662, Apr. 2018.

[24] R. Xue, T. Wang, and H. Tang, "A novel chip pulse employed by ranging code based on simultaneous transmitting CPM modulation and PN ranging in inter-satellite links of GNSS," *IEEE Access*, vol. 8, pp. 132860-132870, Jul. 2020.

[25] X. Zhao, X. Huang, J. Li, K. Zhang, and G. Sun, "Subcarrier periodic shifting BOC modulations," in *China Satellite Navigation Conference (CSNC) 2020 Proc.*: Volume I, Singapore: Springer, Jun. 2020, pp. 517-526.

[26] X. Zhao, X. Huang, Z. Liu, Z. Xiao, and G. Sun, "Improved MBOC modulations based on periodic offset subcarrier," *IET Commun.*, vol. 15, no. 14, pp. 1831-1848, Jul. 2021.

[27] J. Ma, Y. Yang, H. Li, *et al*., "FH-BOC: Generalized low-ambiguity anti-interference spread spectrum modulation based on frequency-hopping binary offset carrier," *GPS Solut.*, vol. 24, pp. 1-16, Apr. 2020.

[28] J. Ma, Y. Yang, L. Ye, L. Deng, and H. Li, "Dual-sideband constant-envelope frequency-hopping binary offset carrier multiplexing modulation for satellite navigation," *Remote Sens.*, vol. 14, no. 16, pp. 3871, Jun. 2022.

[29] J. W. Betz, "Design and performance of code tracking for the GPS M code signal," in *ION Nat. Tech. Meeting*, Salt Lake City, UT, Sep. 2000.

[30] J. A. Avila-Rodriguez, "On generalized signal WFs for satellite navigation," Ph.D. thesis, University FAF Munich, Neubiberg, Germany, 2008.

[31] A. R. Pratt and J. I. R. Owen, "BOC modulation WFs," in *ION Proc., GPS 2003 Conf.*, Portland, Sep. 2003.

[32] J. W. Betz, "Effect of partial-band interference on receiver estimation of C/N0: Theory," in *Proc. Nat. Tech. Meeting of the Inst. Navig. (ION-NTM 2001)*, Long Beach, CA, USA, Jan. 22-24, 2001, pp. 16-27.

[33] J. W. Betz, "The offset carrier modulation for GPS modernization," in *Proc. ION Tech. Meeting*, Jan. 1999, pp. 639–648.

[34] K. Rouabah and D. Chikouche, "GPS/Galileo multipath detection and mitigation using closed-form solutions," *Math. Probl. Eng.*, vol. 2009, pp 1-10, Nov. 2009, doi:10.1155/2009/106870.

[35] S. Titouni, K. Rouabah, S. Atia, M. Flissi, S. Mezaache, and M. S. Bouhlel, "Spectral transformation-based technique for reducing the effect of limited pre-correlation bandwidth in the GNSS receiver filter in presence of noise and multipath," *J. Syst. Eng. Electron.*, vol. 31, no. 2, pp. 252-265, Apr. 2020.

[36] M. Flissi, K. Rouabah, D. Chikouche, A. Mayouf, and S. Atia, "Performance of new BOC-AW-modulated signals for GNSS system," *EURASIP J. Wireless Commun. Netw.*, vol. 2013, pp. 1-18, May. 2013.